Contents

1 Numerical results for the clock model 1
1.1 Introduction 1
1.2 Previous numerical results 3
1.2.1 The $q = 5$ clock model 3
1.2.2 The $q = 6$ clock model 3
1.3 Spectrum of the corner transfer matrix 5
1.4 Magnetization 6
1.5 Classical analogue to the entanglement entropy 6
1.6 Transition temperatures 7
1.6.1 Transition from the ordered to the massless phase T_1 . 9
1.6.2 Transition from the massless to the disordered phase T_2 9
1.7 Central charge of the massless phase 10
1.8 Varying exponent for the magnetization 11
1.9 Discussion 14

Bibliography 15

1
Numerical results for the clock model

We present results of scaling in bond dimension and system size with the CTMRG algorithm for the five- and six-state clock model.

Not finished yet.

1.1 Introduction

In the field of phase transitions and critical phenomena, the two-dimensional topological phase transition discovered by Kosterlitz and Thouless [1, 2] receives much attention. This phase transition is characterized not by an order parameter which indicates a breaking of symmetry, but by the proliferation of topological defects.

In the low-temperature phase, the two-point correlation functions decay with a power-law with varying exponent $\eta(T)$. At the transition, the correlation length diverges as

$$\xi \propto \exp(A|T - T_c|^{-1/2}), \tag{1.1}$$

with A a non-universal constant. Above the transition, the two-point correlators decay exponentially.

The XY model consists of planar rotors on the square lattice. It exhibits the Kosterlitz-Thouless (KT) phase transition and by the Mermin-Wagner-Hohenberg theorem the symmetry of the ground state is broken for all temperatures, due to the $O(2)$ (planar rotational) symmetry of the potential [3, 4].

The q-state clock model possesses the discrete $\mathbb{Z}_q$ symmetry and is an interpolation between the Ising model, which corresponds to $q = 2$, and the XY

model, which corresponds to $q \to \infty$. Its energy function is given by

$$H_q = -\sum_{\langle ij \rangle} \cos(\theta_i - \theta_j), \tag{1.2}$$

with the spins taking the values

$$\theta = \frac{2\pi n}{q} \qquad n \in \{0, \ldots, q-1\}. \tag{1.3}$$

It has been proven that for high enough q, this model indeed exhibits a Kosterlitz-Thouless transition [5]. Furthermore, it has been proven that for $q \geq 5$, a general model with $\mathbb{Z}_q$ symmetry (of which Eq. 1.2 is a special case) has three phases: a symmetry broken phase for $T < T_1$, an intermediate phase with power law decay of the correlation function, and a high-temperature phase with exponential decay of the correlation function for $T > T_2$ [6].

In the Villain formulation of the potential [7], it has been proven that the transition at T_2 is a BK-transition [8], and numerical results suggest that for a broad range of temperatures, the thermodynamic behaviour becomes identical to the XY model for high enough q [9].

Furthermore, in the Villain formulation it is known that [10, 11]

$$\eta(T_1) = \frac{4}{q^2}, \qquad \eta(T_2) = \frac{1}{4}, \tag{1.4}$$

where $\frac{\eta}{2} = \frac{\beta}{\nu}$, the magnetization exponent in the finite-size regime.

For the cosine model in Eq. 1.2, the value q_c for which it first exhibits a BK-transition is not precisely known. There is some disagreement about whether the cases $q = 5, 6$ exhibit KT-type transitions (see previous numerical results below).

In our simulations we will focus on the cases $q = 5, 6$, to (i) study the nature of the phase transition from a new perspective and (ii) compare the accuracy of finite-m and finite-N scaling within the CTMRG method to other established numerical methods.

We briefly summarise previous numerical results, then present results obtained with the CTMRG algorithm.

1.2 Previous numerical results

1.2.1 The $q = 5$ clock model

The general consensus is that the two transitions of the $q = 5$ clock model with cosine potential are of the KT-type, though there are no rigorous results. It is also assumed that the critical indices are the same as those in the Villain formulation.

The disagreement about the nature of the phase transitions stems from numerical results for the helicity modulus [12].

Most notably, Baek and Minnhagen [13] claim that since the helicity modulus does not vanish in the high-temperature phase, the upper transition is not of the KT-type.

It was shown by Kumano et al. in [14], however, that the definition used by Baek and Minnhagen is not suitable for systems with a discrete symmetry. The correct discrete definition yields the expected result, namely that the helicity modulus does vanish and the three-phase KT-picture holds.

The conclusion of Kumano et al, which was obtained by a Monte Carlo study, was verified by Chatelain [15] using the TMRG algorithm [16] (see also **??**). Chatelain also found that the critical indices match those of the Villain model (Eq. 1.4), implying the cosine model is in the same universality class as the Villain model.

After the rebuttal by Kumano et al., Baek et al. published another work [17] in which they again use the (in the eyes of Kumano et al.) wrong definition of the helicity modulus, yet calculated in a different way. Again they conclude the transition is not of the KT-type.

Meanwhile, Borisenko et al. [18] carried out a very detailed Monte Carlo study confirming the KT-picture, using Binder-cumulants to find the critical points and the magnetization and susceptability to find the critical indices.

Brito et al. [19] conclude from a Monte Carlo study that while the transition is of KT-type, the resolution of their numerical method is not high enough to distinguish between T_1 and T_2.

Table 1.1 shows the results for the transition temperatures found by other authors.

1.2.2 The $q = 6$ clock model

Here, there is overwhelming consensus that both transitions are of the KT-type. The only exceptions are Lapilli et al. [9] and Hwang [20].

Lapilli et al. use the incorrect definition of the helicity modulus.

	T_1	T_2
Brito et al.[1] (2010) [19]	0.91	0.90
Borisenko et al. (2011) [18]	0.9056	0.9432
Kumano et al. (2013) [14]	0.908	0.944
Chatelain (2014) [15]	0.914	0.945
This work (finite-N scaling)	0.915	0.935
This work (finite-m scaling)	-	0.944

Table 1.1: Previous results for the transition temperatures for $q = 5$.

	T_1	T_2
Tomita and Okabe (2002) [22]	0.7014	0.9008
Hwang[2] (2009) [20]	0.632	0.997
Brito et al. (2010) [19]	0.68	0.90
Kumano et al. (2013) [14]	0.700	0.904
Krčmár et al. (2016) [21]	0.70	0.88
This work (finite-N scaling)	-	-
This work (finite-m scaling)	-	-

Table 1.2: Previous results for the transition temperatures for $q = 6$.

Hwang asserts that the transition is not of KT-type because the data, which was obtained from systems of rather small size ($L \times L$-systems with $L = 20, \ldots, 28$), also agrees with a power-law divergence of the correlation length. We will get back to this point.

The previous results for the transition temperatures are listed in Table 1.2. For an overview that goes further back, see [21].

We note that [14, 19, 22] use Monte Carlo methods, while [21] uses the CTMRG algorithm (combined with finite-size scaling, but not with finite-m scaling).

[1] These authors found $T_1 > T_2$, which is not an error in the text, but due to the low resolution of the methods used.

[2] To obtain these values, the author assumed an algebraic divergence of the correlation length.

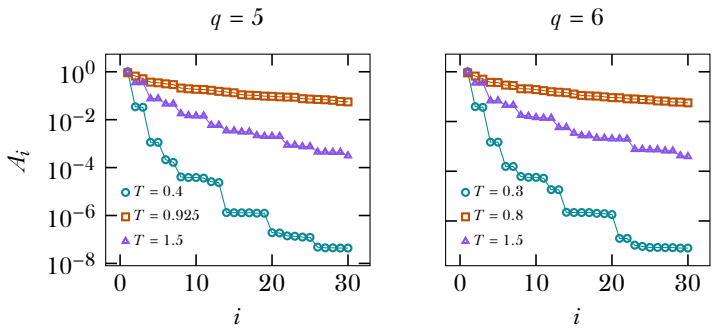

Figure 1.1: First part of the spectrum of A with fixed boundary, calculated with $m = 100$ and a convergence threshold of 10^{-8}, at temperatures corresponding to the ordered phase, approximate midpoint of the massless phase and disordered phase, respectively.

1.3 Spectrum of the corner transfer matrix

In order to get an idea of the accuracy that we might expect, we have plotted the spectrum of the $q = \{5, 6\}$ clock models in Fig. 1.1.

It is clear that the spectra of both clock models fall off at about the same pace, if we compare points in the ordered, massless and disordered phase. The $q = 6$ clock model has a slightly more degenerate spectrum, as might be expected from its larger symmetry group, but there is no clear pattern.

As compared to the Ising model (see ??), the spectra of the $q = \{5, 6\}$ clock models fall off much more slowly[3]. This implies that a much larger bond dimension is needed to obtain the same accuracy for quantities in the thermodynamic limit.

[3]For the calculation of the spectrum of the Ising model in this work, a bond dimension of $m = 250$ was used, as opposed to $m = 100$ for the clock model. This means that, in small part, the slower decay of the spectrum is due to the normalization $\mathrm{Tr}\, A^4 = 1$. But this does not change the general picture that the spectra of the $q = \{5, 6\}$ clock models decay more slowly.

1.4 Magnetization

For the clock model, we define the magnetization per site as

$$M = \langle \cos \theta_0 \rangle, \tag{1.5}$$

where θ_0 is the central spin.

This quantity can be computed in the same way as for the Ising model (see ??) by generalizing the tensor b_{ijkl} to

$$b_{ijkl} = \sum_{n \in \{0,\ldots,q-1\}} \cos\left(\frac{2\pi n}{q}\right) \delta_{nijkl}. \tag{1.6}$$

1.5 Classical analogue to the entanglement entropy

The classical analogue to the half-chain entanglement entropy S is defined in ??. Its definition remains valid.

In the limit $T \to \infty$, for both a fixed and free boundary, we have

$$S(T \to \infty) = 0. \tag{1.7}$$

To see this, consider that all 2^2N configurations on the inner edges of the $N \times N$ quadrant represented by the corner transfer matrix are equally likely in this limit, hence

$$A_{ij} = \frac{1}{2^{2N}} \tag{1.8}$$

which is matrix with one eigenvalue of 1 and the others 0[4].

In the limit $T \to 0$, there is only one non-zero matrix element in the case of a fixed boundary (namely all inner spins having the same value as the outer boundary), and q equally likely configurations in the case of a free boundary, yielding

$$S^{\text{fixed}}(T = 0) = 0,$$
$$S^{\text{free}}(T = 0) = \log q.$$

[4] One can also make the argument that the corresponding quantum state tends to a product state in the limit $T \to 0$, yielding the same conclusion.

For a fixed boundary, the point of maximum entropy approaches the massless phase from the high-temperature region, hence tending towards T_2. In contrast, the point of maximum entropy approaches T_1 for systems with a free boundary.

Maybe make intuitive why?

Fig. 1.2 shows these quantities for $q = 5$ for systems with a fixed boundary.

Finish this paragraph when results of $q = 6$ are in.

1.6 Transition temperatures

Since we expect an essential singularity of the form in Eq. 1.1 for both transition temperatures, for finite systems we have

$$N = a \exp\left(b|T^\star(N) - T_c|^{-1/2}\right), \tag{1.9}$$

where N is an effective finite length scale of the system and a and b are non-universal constants. N is the system size in the case of finite-size scaling and a length scale derived from the bond dimension m in the case of finite-m scaling.

We define $T^\star(N)$ as the point of maximum entanglement entropy, as discussed in ??.

Inverting Eq. 1.9 gives the following relations for the pseudocritical transition temperatures

$$T_1^\star(N) = -\frac{\alpha_1}{(\log \beta_1 N)^2} + T_1 \tag{1.10}$$

$$T_2^\star(N) = \frac{\alpha_2}{(\log \beta_2 N)^2} + T_2 \tag{1.11}$$

where $\alpha = b^2$ and $\beta = 1/a$ (we drop the subscripts denoting the transition).

For convenience, we define the scaled length variable

$$\ell = (\log \beta N)^2, \tag{1.12}$$

such that

$$T^\star(N) - T_c \propto \frac{1}{\ell}. \tag{1.13}$$

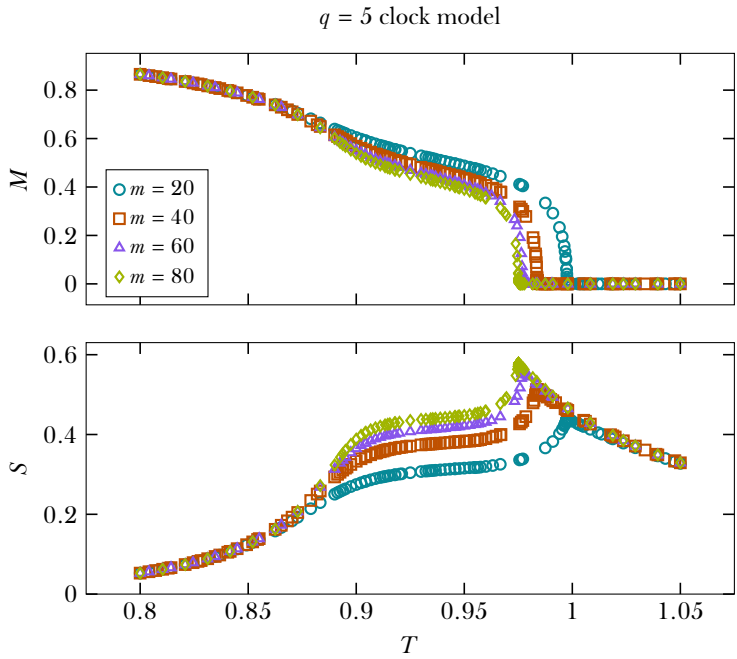

Figure 1.2: Classical analogue to half chain entanglement entropy (??) and magnetization (Eq. 1.5) computed for systems with a fixed boundary for the $q = 5$ clock model. Simulations were done with a convergence threshold of 10^{-7}.

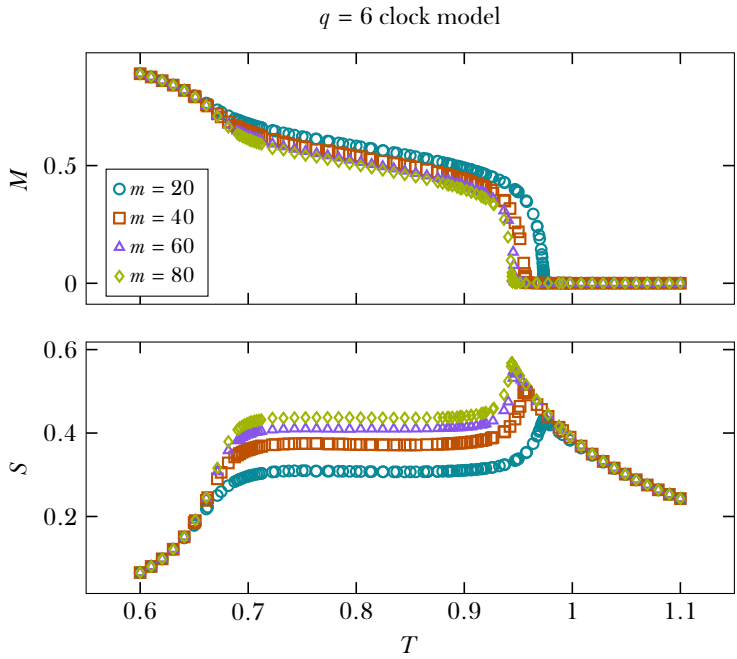

Figure 1.3: Classical analogue to half chain entanglement entropy (??) and magnetization (Eq. 1.5) computed for systems with a fixed boundary for the $q = 6$ clock model. Simulations were done with a convergence threshold of 10^{-7}.

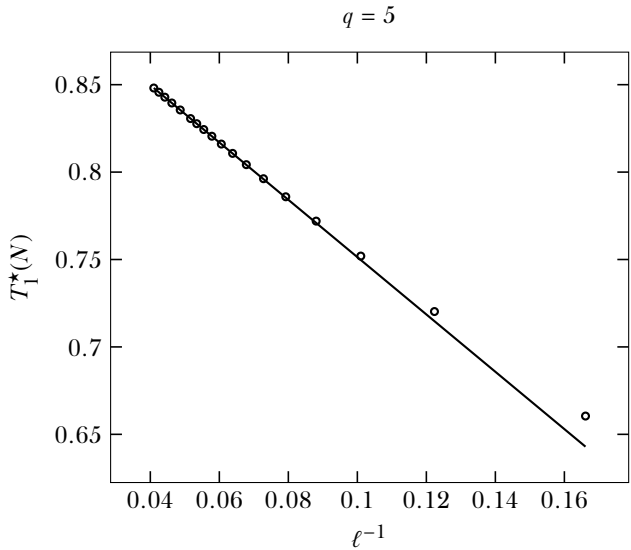

Figure 1.4: We find $T_1 = 0.915$ for the $q = 5$ clock model. We have fitted the final 8 points $n = \{60, 65, 70, 80, 90, 100, 110, 120\}$. m was chosen such that the truncation error was smaller than 10^{-6} for $n \leq 70$ and smaller than 10^{-5} for $n > 70$. In finding the maximum of the entropy, a tolerance in temperature of 10^{-5} was used.

1.6.1 Transition from the ordered to the massless phase T_1

Say what length scale is used in case of finite-m

1.6.2 Transition from the massless to the disordered phase T_2

- talk about how structure makes it hard to fit finite-m data, but it simulates much larger systems, thus yielding much better results.

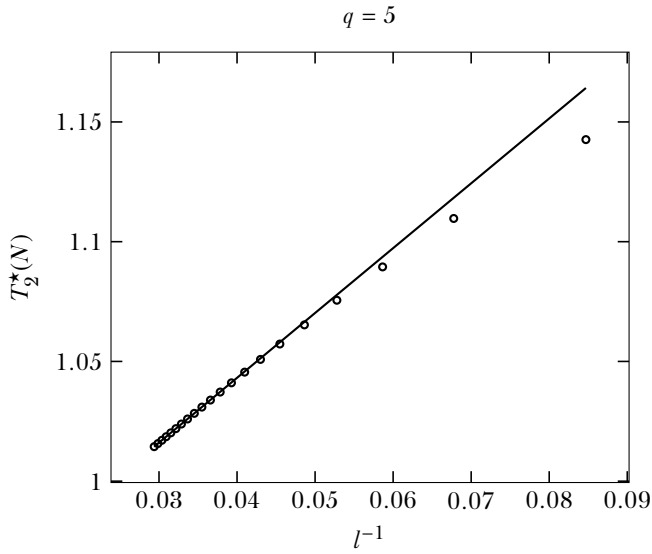

Figure 1.5: We find $T_1 = 0.935$ for the $q = 5$ clock model with finite-size scaling. We have fitted the final 6 points $n = \{85, 90, \ldots, 110\}$. m was chosen such that the truncation error was smaller than 10^{-6}. In finding the maximum of the entropy, a tolerance in temperature of 10^{-6} was used.

1.7 Central charge of the massless phase

Since the massless phase corresponds to a Gaussian model, we expect the central charge to be 1 there [2].

By fitting the relation

$$S \propto \frac{c}{6} \log \xi(m), \tag{1.14}$$

where $\xi(m)$ is calculated as in ??, we can directly extract the central charge in this region.

The result is shown in the top panel of Fig. 1.6. It is seen to precisely agree with $c = 1$ in the massless phase.

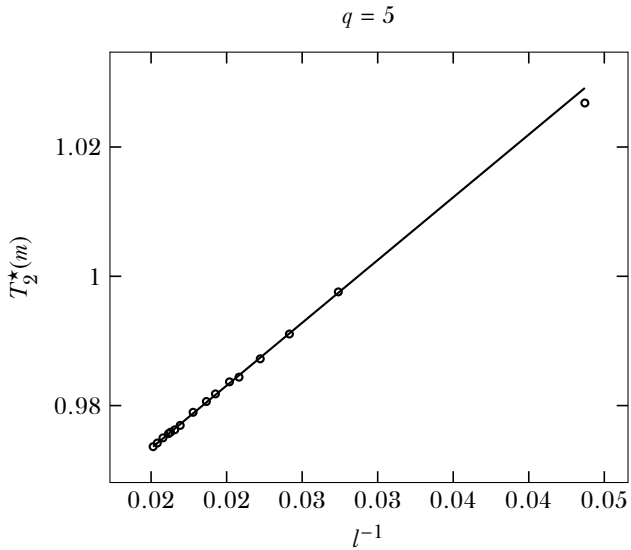

Figure 1.6: For the finite-m simulations, the fit yields $T_2 = 0.944.$ using $m = 20, 25, \ldots, 90$ with a convergence threshold of 10^{-7}. The pseudocritical temperature belonging to $m = 10$ is also shown, but is not included in the fit.

Outside the massless phase, a good fit to Eq. 1.14 can no longer be obtained. This is consistent with the location of T_1 and T_2 that are found in this work.

1.8 Varying exponent for the magnetization

We may verify the exponent with which the magnetization goes to zero in the massless phase by fitting

$$M(m, T) = \xi(m)^{-\frac{\eta(T)}{2}}, \tag{1.15}$$

where we defined $\xi(m)$ via Eq. 1.14.

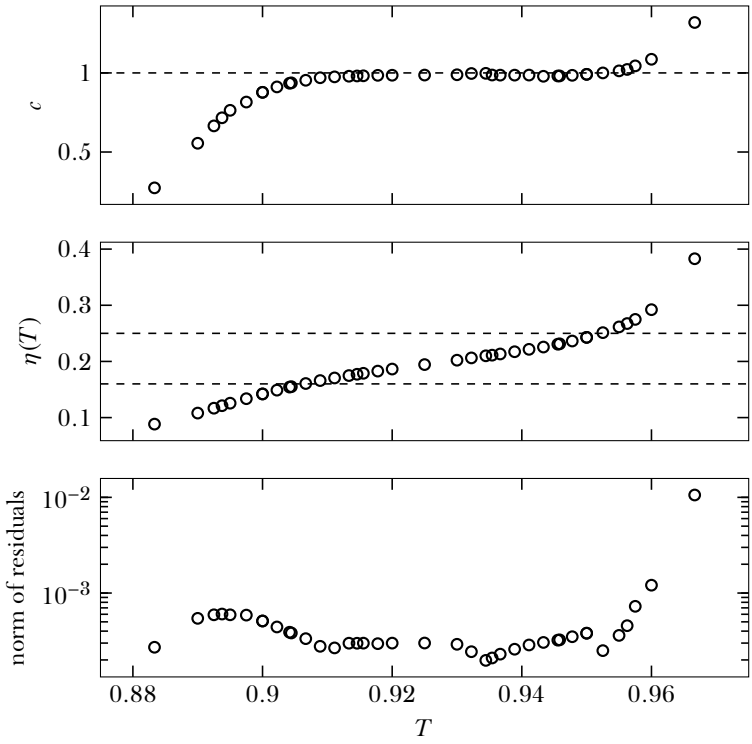

Figure 1.7: $\frac{2\beta}{\nu}$ reaches $\frac{4}{25}$ around $T = 0.906$ and $\frac{1}{4}$ around $T = 0.952$. First 4 values were left out of the fit.

The result is shown in the middle panel of Fig. 1.6. It agree very well with bla bla. Refer to villain exponents.

Finish this when T_1 is definite

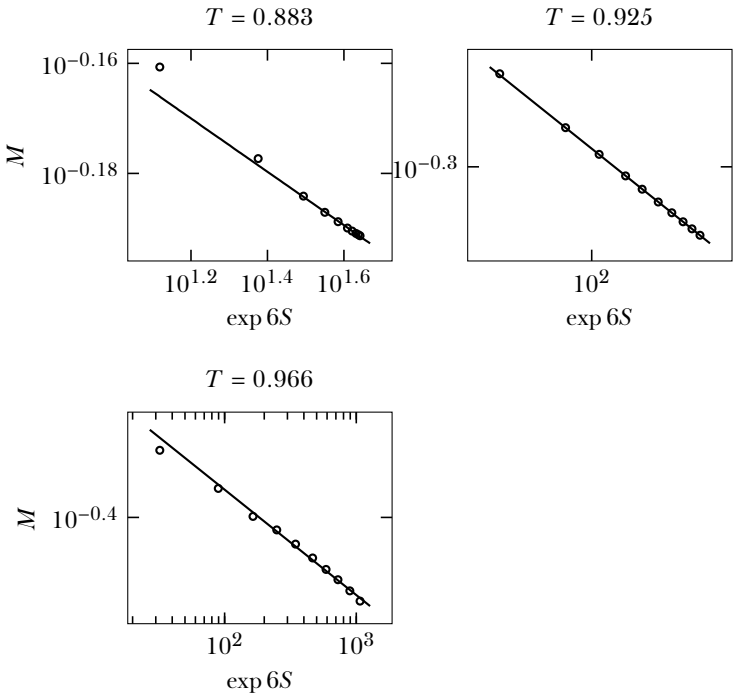

Figure 1.8: Fits to Eq. 1.15 for temperatures a little bit to the left of, in the middle of and a little bit to the right of the massless phase, respectively.

1.9 Discussion

- doesn't apparently make sense to take many consecutive m-values. Rather take sparse, but bigger m-values.
- For finite-N: tradeoff between truncation error and finite-size effects are not clear.
- finite-χ reaches much bigger system sizes, but has structure that needs to be overcome while fitting.
- fix bug where I attached an a-tensor with wrong temperature.
- omitting m values seems to give worse results than just taking them all, except for the really small ones.
- second-order phase transition cannot be ruled on grounds of this data, but is there theory that forbids it?
- If you make convergence too low, it can get impossible to reach, even for fixed boundary?

Bibliography

[1] J. M. Kosterlitz, and D. J. Thouless, "Ordering, metastability and phase transitions in two-dimensional systems", Journal of Physics C: Solid State Physics **6**, 1181 (1973).

[2] J. M. Kosterlitz, "The critical properties of the two-dimensional xy model", Journal of Physics C: Solid State Physics **7**, 1046 (1974).

[3] N. D. Mermin, and H. Wagner, "Absence of ferromagnetism or antiferromagnetism in one-or two-dimensional isotropic Heisenberg models", Physical Review Letters **17**, 1133 (1966).

[4] P. C. Hohenberg, "Existence of long-range order in one and two dimensions", Physical Review **158**, 383 (1967).

[5] J. Fröhlich, and T. Spencer, "The Kosterlitz-Thouless transition in two-dimensional abelian spin systems and the Coulomb gas", Communications in Mathematical Physics **81**, 527–602 (1981).

[6] J. Cardy, "General discrete planar models in two dimensions: duality properties and phase diagrams", Journal of Physics A: Mathematical and General **13**, 1507 (1980).

[7] J. Villain, "Theory of one-and two-dimensional magnets with an easy magnetization plane. II. the planar, classical, two-dimensional magnet", Journal de Physique **36**, 581–590 (1975).

[8] J. V. José, L. P. Kadanoff, S. Kirkpatrick, and D. R. Nelson, "Renormalization, vortices, and symmetry-breaking perturbations in the two-dimensional planar model", Physical Review B **16**, 1217 (1977).

[9] C. M. Lapilli, P. Pfeifer, and C. Wexler, "Universality away from critical points in two-dimensional phase transitions", Physical Review Letters **96**, 140603 (2006).

[10] S. Elitzur, R. B. Pearson, and J. Shigemitsu, "Phase structure of discrete abelian spin and gauge systems", Physical Review D **19**, 3698–3714 (1979).

[11] B. Nienhuis, "Critical behavior of two-dimensional spin models and charge asymmetry in the Coulomb gas", Journal of Statistical Physics **34**, 731–761 (1984).

[12] M. E. Fisher, M. N. Barber, and D. Jasnow, "Helicity modulus, superfluidity, and scaling in isotropic systems", Physical Review A **8**, 1111–1124 (1973).

[13] S. K. Baek, and P. Minnhagen, "Non-Kosterlitz-Thouless transitions for the q-state clock models", Physical Review E **82**, 031102 (2010).

[14] Y. Kumano, K. Hukushima, Y. Tomita, and M. Oshikawa, "Response to a twist in systems with Z_p symmetry: the two-dimensional p-state clock model", Physical Review B **88**, 104427 (2013).

[15] C. Chatelain, "DMRG study of the Berezinskii–Kosterlitz–Thouless transitions of the 2D five-state clock model", Journal of Statistical Mechanics: Theory and Experiment **2014**, P11022 (2014).

[16] T. Nishino, "Density matrix renormalization group method for 2D classical models", Journal of the Physical Society of Japan **64**, 3598–3601 (1995).

[17] S. K. Baek, H. Mäkelä, P. Minnhagen, and B. J. Kim, "Residual discrete symmetry of the five-state clock model", Physical Review E **88**, 012125 (2013).

[18] O. Borisenko, G. Cortese, R. Fiore, M. Gravina, and A. Papa, "Numerical study of the phase transitions in the two-dimensional $Z(5)$ vector model", Physical Review E **83**, 041120 (2011).

[19] A. F. Brito, J. A. Redinz, and J. A. Plascak, "Two-dimensional XY and clock models studied via the dynamics generated by rough surfaces", Physical Review E **81**, 031130 (2010).

[20] C.-O. Hwang, "Six-state clock model on the square lattice: Fisher zero approach with Wang-Landau sampling", Physical Review E **80**, 042103 (2009).

[21] R. Krčmár, A. Gendiar, and T. Nishino, "Phase transition of the six-state clock model observed from the entanglement entropy", arXiv:1612.07611 (2016).

[22] Y. Tomita, and Y. Okabe, "Probability-changing cluster algorithm for two-dimensional XY and clock models", Physical Review B **65**, 184405 (2002).